Materials Today Bio 25 (2024) 101020

Contents lists available at ScienceDirect

Materials Today Bio

journal homepage: www.journals.elsevier.com/materials-today-bio

Primary adipocytes as targetable drug depot to prevent post-surgical cancer recurrence

Yang Bo [a], Yueji Wang [a,b], Joonsu Han [a], Rimsha Bhatta [a], Yusheng Liu [a], Dhyanesh Baskaran [a], Jiadiao Zhou [a], Hua Wang [a,c,d,e,f,g,h,*]

[a] Department of Materials Science and Engineering, University of Illinois at Urbana-Champaign, Urbana, IL, 61801, USA
[b] Department of Mechanical Science and Engineering, University of Illinois at Urbana-Champaign, Urbana, IL, 61801, USA
[c] Cancer Center at Illinois (CCIL), Urbana, IL, 61801, USA
[d] Department of Bioengineering, University of Illinois at Urbana-Champaign, Urbana, IL, 61801, USA
[e] Carle College of Medicine, University of Illinois at Urbana-Champaign, Urbana, IL, 61801, USA
[f] Beckman Institute for Advanced Science and Technology, University of Illinois at Urbana-Champaign, Urbana, IL, 61801, USA
[g] Materials Research Laboratory, University of Illinois at Urbana-Champaign, Urbana, IL, 61801, USA
[h] Institute for Genomic Biology, University of Illinois at Urbana-Champaign, Urbana, IL, 61801, USA

ARTICLE INFO

Keywords:
Adipocyte
Fat tissue
Metabolic glycan labeling
Click chemistry
Breast cancer

ABSTRACT

Surgery followed by adjuvant chemotherapy or radiation therapy remains the mainstream treatment for breast cancer in the clinic. However, cancer recurrence post surgery is still common. In view of the clinical practice that autologous fat tissue grafting is often used to facilitate breast reconstruction after lumpectomy, here we develop an *in vivo* targetable adipocyte-based drug depot for the prevention of post-surgical cancer recurrence. We show that primary adipocytes can be metabolically labeled with clickable chemical tags (e.g., azido groups), for subsequent conjugation of dibenzocyclooctyne (DBCO)-bearing cargo via efficient click chemistry. The conjugated cargo can retain well on the adipocyte membrane. By incorporating a cleavable linker between DBCO and cargo, the conjugated cargo can be gradually released from the surface of adipocytes to effect on neighboring cells. In the context of breast cancer surgery, azido-labeled adipocytes grafted to the surgical site can capture circulating DBCO-drugs for improved prevention of 4T1 triple-negative breast cancer (TNBC) recurrence and metastasis. This targetable and refillable adipocyte-based drug depot holds great promise for drug delivery, transplantation, and other applications.

1. Introduction

Breast cancer is the most common cancer diagnosed in women, with surgery followed by either adjuvant chemotherapy or radiation therapy remaining the mainstream treatment in the clinic [1,2]. In particular, triple-negative breast cancer (TNBC), a subtype of breast cancer negative for human epidermal growth factor receptor 2 (HER2), estrogen receptor, and progesterone receptor, is notorious for the lack of targeted therapies and high recurrence rates [3]. Surgery, coupled with chemotherapy or radiation therapy, remains the mainstream treatment for TNBC [4]. In spite of postoperative interventions, tumor recurrence after the surgical resection of TNBC is still not uncommon [5,6]. Among different factors, the residual cancer cells at the surgical site after lumpectomy could be a key contributor to tumor recurrence [7,8]. A variety of strategies have been explored to reduce the risk of breast cancer recurrence. For example, hydrogels that facilitate the controlled release of chemotherapeutics were implanted at the surgical site to clear residual tumor cells [9,10]. The co-loading of chemotherapeutics and immune-stimulatory agents has also been used to induce the immunogenic death of cancer cells and elicit an antitumor cytotoxic T lymphocyte (CTL) response [11,12]. Additionally, local administration of radioisotopes coupled with radiation has been deployed to control residual tumor cells and prevent tumor recurrence [13,14]. While these approaches can introduce drugs during the surgery, the key challenge lies in the ability to deliver anticancer drugs to the tumor resection site whenever needed post surgery, especially considering that postoperative chemotherapy is often recommended for patients with high risks of cancer recurrence.

* Corresponding author. Department of Materials Science and Engineering, University of Illinois at Urbana-Champaign, Urbana, IL, 61801, USA.
E-mail address: huawang3@illinois.edu (H. Wang).

https://doi.org/10.1016/j.mtbio.2024.101020
Received 4 November 2023; Received in revised form 1 March 2024; Accepted 6 March 2024
Available online 7 March 2024

In clinical practice, to aid breast reconstruction, autologous fat tissues are often grafted to the surgical site during lumpectomy [15–17]. We envision approaches that can take advantage of the fat tissue graft to deliver drugs and manage the residual cells hold promise to reduce the risk of tumor recurrence [18,19]. Adipose tissues are abundant in the body, can be easily identified and isolated, and are minimally immunogenic, providing an ideal source of biocompatible materials for drug delivery and transplantation applications [17]. While drugs can be adsorbed to fat tissues at the time of surgery, methods to target drugs to fat tissues grafted to the surgical site *in vivo* are still lacking [20,21]. Metabolic glycan labeling provides a powerful pool to introduce unique chemical tags (e.g., azido groups) to cell membranes via metabolic glycoengineering processes of unnatural sugars [22–25], for subsequent targeted conjugation of dibenzocyclooctyne (DBCO)-bearing agents via efficient and bioorthogonal click chemistry [26,27]. While metabolic glycan labeling has been actively applied to labeling and targeting of cancer cells, immune cells, and bacteria [22–25,28–31], metabolic labeling of primary cells, especially lowly-proliferative primary adipocytes has not been reported thus far.

Here we show that primary murine adipocytes can be successfully metabolically labeled with chemical tags (e.g., azido groups) via the metabolic glycan labeling technology. In compliance with the clinical practice, we demonstrate that by incubating freshly isolated primary adipocytes with azido-sugars for 2 h and injecting them into the mammary fat pad of mice, the adipocytes managed to continue the metabolic glycan labeling process and express azido groups on the cell membrane *in vivo*. Further, we demonstrate that azido-labeled primary adipocytes, upon grafting to the tumor resection site, can capture circulating DBCO-drugs *in vivo* via efficient click chemistry. By incorporating a degradable linkage between DBCO and drug, the conjugated drugs can be gradually released from adipocyte membranes to effect on the neighboring residual tumor cells, for the improved prevention of tumor recurrence and metastasis in a 4T1 triple negative breast cancer model (Fig. 1). As a proof-of-concept demonstration, we used DBCO-functionalized platin as a representative chemotherapeutics to demonstrate adipocyte targeting and subsequent controlled release. This targeting approach is widely applicable to other types of chemotherapeutics.

2. Results

2.1. In vivo metabolic labeling of primary adipocytes

We first studied whether primary adipocytes could be metabolically labeled with azido groups via the metabolic glycoengineering process of tetraacetyl-*N*-azidoacetylmannosamine (Ac_4ManNAz), a commonly used labeling agent. Fat tissues were harvested from the abdominal fat pad of Balb/c mice, following a method previously described [32]. To fit into the clinical process of fat tissue grafting in the context of breast cancer surgery where fat tissues are rapidly harvested and transplanted, we incubated the harvested adipocytes in the solution of Ac_4ManNAz for 2 h before transplanting into the left mammary fat pad of Balb/c mice. For comparison, adipocytes without Ac_4ManNAz treatment were injected into the right mammary fat pad as the control. Adipocytes were also stained with Calcein AM for fluorescence tracing of cells. At 48 h post-transplantation, the fat tissues were collected for the detection of cell-surface azido groups using DBCO-Cy5 via click chemistry (Fig. 2a). ~27 % of isolated cells were Calcein AM-positive, which correspond to the injected adipocytes (Fig. S1). Among the Calcein AM^+ population (adoptively transferred adipocytes), Ac_4ManNAz-pretreated adipocytes showed higher Cy5 fluorescence intensity than their untreated counterparts, demonstrating the successful metabolic labeling of primary adipocytes with azido groups (Fig. 2b–d). Confocal imaging of the harvested adipocytes also validated the increased accumulation of Cy5 in Ac_4ManNAz-pretreated adipocytes than in the control adipocytes

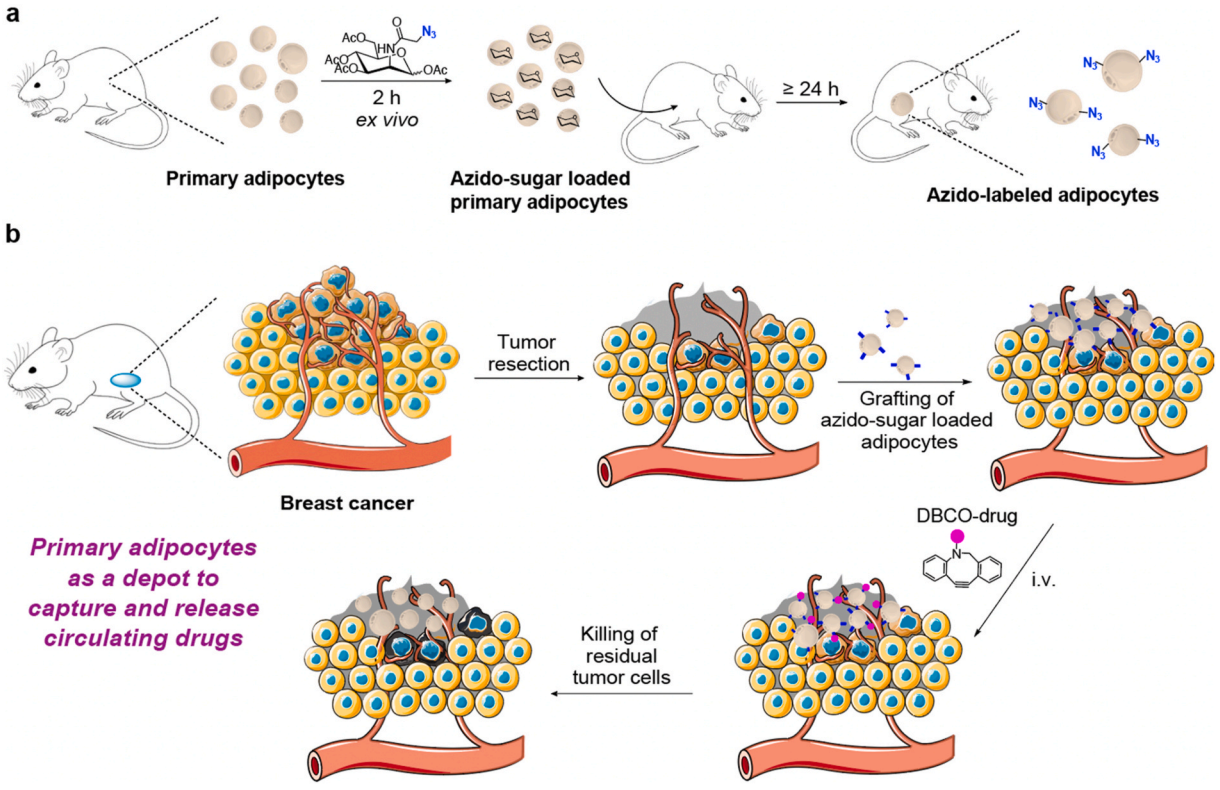

Fig. 1. Schematic illustration of metabolic labeling and targeting of primary adipocytes for post-surgical prevention of tumor recurrence. (a) Primary adipocytes can be loaded with azido-sugars, and upon grafting into mice, become metabolically labeled with azido groups. (b) In the context of breast cancer surgery, azido-sugar loaded adipocytes grafted to the surgical site can mediate targeted conjugation of systemically administered DBCO-drugs via click chemistry, leading to improved prevention of 4T1 TNBC recurrence and metastasis.

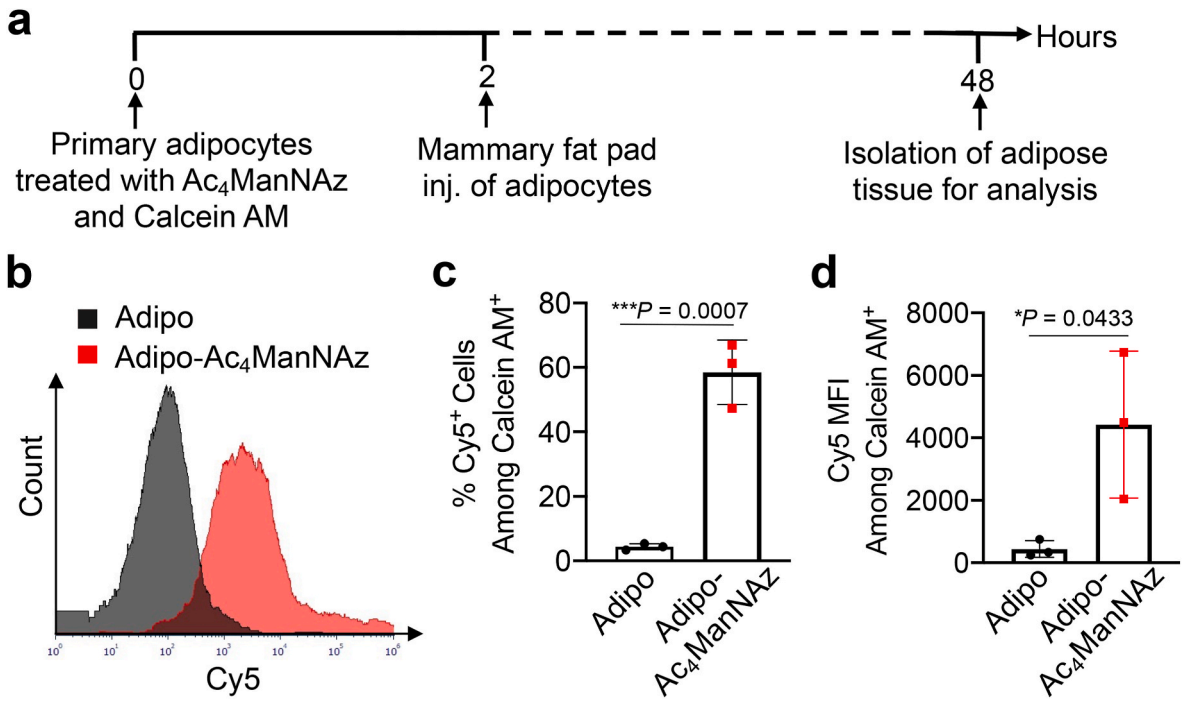

Fig. 2. Metabolic labeling of primary adipocytes. (a–d) Primary adipocytes were isolated, incubated with $Ac_4ManNAz$ and Calcein AM for 2 h, and transplanted into the mammary fat pad of Balb/c mice. After 48 h, grafted fat tissues were retrieved for analysis. (a) Timeframe of the study. (b) Representative Cy5 histograms of retrieved primary adipocytes after incubation with DBCO-Cy5 for 30 min. Calcein AM^+ cells were pre-gated. (c) Percentage of $Cy5^+$ cells and (d) mean Cy5 fluorescence intensity of cells among the retrieved Calcein AM^+ adipocytes. All the numerical data are presented as mean ± SD and analyzed by two-tailed Welch's *t*-test ($0.01 < {}^*P \leq 0.05$; $0.001 < {}^{**}P \leq 0.01$; $0.0001 < {}^{***}P \leq 0.001$, $^{****}P \leq 0.0001$).

(Fig. S2). These experiments demonstrated that primary adipocytes, after short-term incubation in a solution of azido-sugars prior to grafting, can continue the metabolic labeling process after transplantation and become metabolically labeled with azido groups *in vivo*.

2.2. *In vivo targeting of primary adipocytes*

We next studied whether the azido-labeled primary adipocytes can mediate targeted delivery of DBCO-cargo via click chemistry *in vivo*. Primary adipocytes were treated with $Ac_4ManNAz$ or PBS for 2 h and grafted to the left and right mammary fat pad of Balb/c mice, respectively. After 48 h, DBCO-Cy5 was intravenously administrated (Fig. 3a). At 24 h post-injection of DBCO-Cy5, IVIS imaging of mice revealed a much higher Cy5 accumulation in the $Ac_4ManNAz$-treated fat tissues than the control fat tissues (Fig. 3b). This phenomenon was consistent across all individual mice (Fig. 3c). Quantitative analysis of Cy5 fluorescence intensity indicated a ~2.0-fold Cy5 signal in the $Ac_4ManNAz$-treated fat tissues in comparison with the control fat tissues (Fig. 3c–d). *Ex vivo* imaging of the harvest fat tissues also confirmed higher Cy5 accumulation in $Ac_4ManNAz$-treated fat tissues than in the control fat tissues (Fig. 3e), with a ~2.5-fold Cy5 accumulation in the $Ac_4ManNAz$-treated fat tissues (Fig. 3f–g). As DBCO-Cy5 was intravenously injected, it is normal to see the accumulation of DBCO-Cy5 in organs such as liver and kidney (Fig. 3e). These experiments demonstrated that azido-labeled primary adipocytes can mediate targeted conjugation of DBCO-cargo via click chemistry *in vivo*.

2.3. *Azido-labeled adipocytes enable conjugation of DBCO-drug*

After demonstrating that primary adipocytes can be metabolically labeled with azido groups for subsequent targeted conjugation of DBCO-Cy5, we next studied whether azido-labeled adipocytes can covalently capture DBCO-functionalized drugs. Cisplatin, a first-line chemodrug for treating breast cancer [33], was mainly studied. Cisplatin was oxidized by hydrogen peroxide and conjugated with succinic anhydride to yield a carboxyl-bearing prodrug, which was then conjugated with DBCO-amine to yield DBCO-platin-OH (Fig. 4a). Octyl isocyanate was then reacted with the hydroxyl group of DBCO-platin-OH to yield DBCO-platin with a hydrophobic octyl group, which was shown to increase the stability of platin structure (Fig. 4a) [34]. The synthesized DBCO-platin was characterized by NMR and mass spectrometry (Fig. S3). DBCO-platin was stable under physiological conditions, but could be rapidly degraded into cisplatin in the presence of reductives such as ascorbate (Fig. 4b–c) [35,36]. MTT assay revealed an IC_{50} value of 12.4 μM and 0.4 μM for DBCO-platin and cisplatin, respectively against 4T1 TNBC (Fig. 4d). The cytotoxicity of DBCO-platin and cisplatin on 3T3-L1 differentiated adipocytes were also evaluated via the MTT assay (3T3-L1-differentiated adipocytes were used because of the difficulty in long-term *in vitro* culture of primary adipocytes [37]), which showed an IC50 value of 42.3 μM for DBCO-platin and 4.5 μM for cisplatin (Fig. 4e). It is noteworthy that ~100% of cells showed the lipid droplet structure at 7–10 days post the differentiation of 3T3-L1 cells, which was confirmed by Nile Red staining (Figs. S4a–c), indicating the high purity of the differentiated adipocytes. Small-molecule DBCO-platin, if not covalently conjugated to adipocytes, can be internalized via endocytosis and become degraded by the abundant intracellular reductases and other reductives into free platin, which can then induce the crosslinking of DNA and the death of cells. These data demonstrated that adipocytes have a significantly lower sensitivity to both DBCO-platin and cisplatin compared to 4T1 cancer cells. To confirm whether 3T3-L1-differentiated adipocytes can be metabolically labeled with azido groups via $Ac_4ManNAz$ treatment, we incubated them with $Ac_4ManNAz$ for 72 h, followed by the staining with DBCO-Cy5. $Ac_4ManNAz$-treated adipocytes showed a uniform Cy5 signal on the cell membrane (Fig. S5), confirming the successful metabolic azido tagging. To study whether DBCO-platin can be conjugated to azido-labeled adipocytes, 3T3-L1-differentiated adipocytes were pre-treated with $Ac_4ManNAz$ or PBS for three days and then incubated with

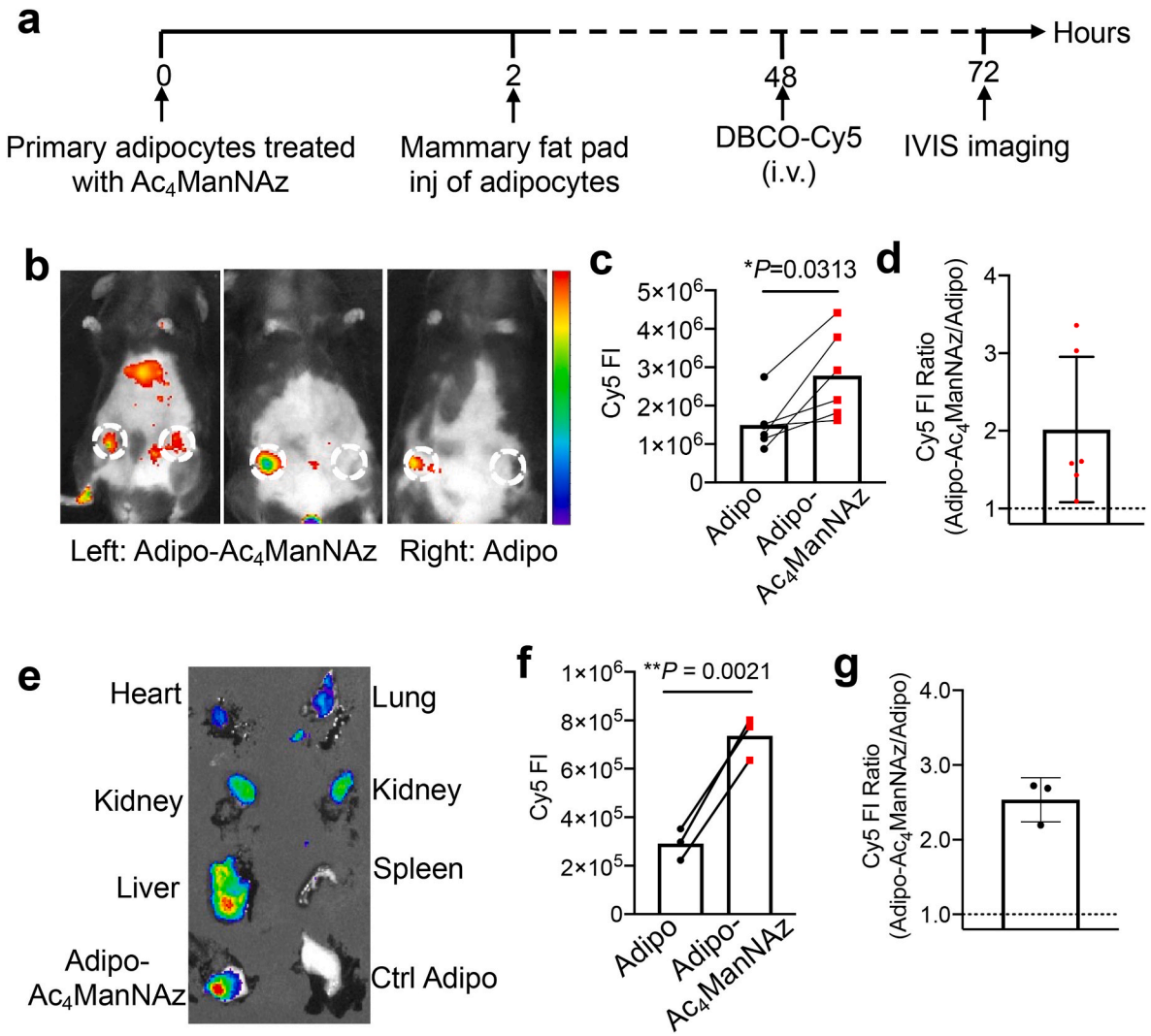

Fig. 3. ***In vivo*** **targeting of primary adipocytes.** Primary adipocytes were incubated with Ac_4ManNAz for 2 h, and transplanted into the left mammary fat pad of Balb/c mice. Control adipocytes treated with PBS were transplanted into the right mammary fat pad. After 48 h, DBCO-Cy5 was intravenously injected. (a) Timeframe of the study. (b) Representative *in vivo* fluorescence imaging of mice at 24 h post injection of DBCO-Cy5. (c) Cy5 fluorescence intensity of fat tissues pretreated with Ac_4ManNAz or PBS. (d) Ratio of Cy5 fluorescence intensity from (c). (e) Representative *ex vivo* fluorescence imaging of harvested tissues. (f) Cy5 fluorescence intensity of harvested adipose tissues pretreated with Ac_4ManNAz or PBS. (g) Ratio of Cy5 fluorescence intensity from (f). All the numerical data are presented as mean ± SD and analyzed by two-tailed student's t-test ($0.01 < {}^{*}P \leq 0.05$; $0.001 < {}^{**}P \leq 0.01$; $0.0001 < {}^{***}P \leq 0.001$, $^{****}P \leq 0.0001$).

DBCO-platin. After removing the unbounded prodrug, cells were lysed and treated with nitric acid prior to the quantification of platinum by ICP-MS (Fig. 4f). A higher accumulation of DBCO-platin in Ac_4ManNAz-treated adipocytes than control adipocytes was detected (Fig. 4f), demonstrating the successful capture of DBCO-platin by azido-labeled adipocytes.

2.4. *Drug-conjugated adipocytes can release drugs to effect on cancer cells*

After demonstrating that DBCO-platin can be conjugated onto azido-labeled adipocytes, we next studied whether the conjugated platin can be gradually released from adipocytes to kill surrounding cancer cells. In a co-culture study, we seeded platin-conjugated adipocytes, obtained via the incubation of Ac_4ManNAz-treated adipocytes with DBCO-platin (25 μM) for 1 h, in a transwell insert and placed 4T1 cancer cells below the transwell (Fig. 4g). Based on the conjugation efficiency of DBCO-platin onto azido-labeled adipocytes (Fig. 4f), the overall concentration of platin being conjugated to adipocytes is ~0.05 μM. Ideally, the conjugated platin can be released from the adipocytes and induce the killing of cancer cells. Considering that cisplatin has an IC_{50} value of 0.4 μM against 4T1 cancer cells and 4.5 μM against adipocytes (Fig. 4d–e), the dose of DBCO-platin (0.05 μM) used in this co-culture study should be safe to adipocytes, ruling out the concern of drug-induced killing of adipocytes. At 72 h post co-culcutre, 4T1 cells co-cultured with platin-conjugated adipocytes exhibited a slightly lower viability than control 4T1 cells (Fig. 4h). At 96 or 120 h, compared to 4T1 cells treated with PBS for control adipocytes, 4T1 cells treated with platin-conjugated adipocytes consistently exhibited significantly lower viability (Fig. 4h), indicating that covalently conjugated platin can be gradually released from adipocytes to induce the death of neighboring cancer cells. It is possible that adipocytes may experience apoptosis or death over an extended culture time (e.g., 120 h), the comparison between the adipocyte and platin-conjugated platin groups still indicated the contribution of platin to the enhanced killing of 4T1 cancer cells. To further validate platin-induced cytotoxic effects against cancer cells, we co-incubated 4T1 cells with platin-conjugated adipocytes (Adipo-N_3+DBCO-Platin), adipocyte alone, DBCO-platin alone, or PBS for 72 h, followed by the staining of intracellular phospho-Histone H2A.X (pH2A.X) in 4T1 cells [38]. Compared to 4T1 cells treated with adipocyte alone or PBS, 4T1 cells treated with platin-conjugated adipocytes or

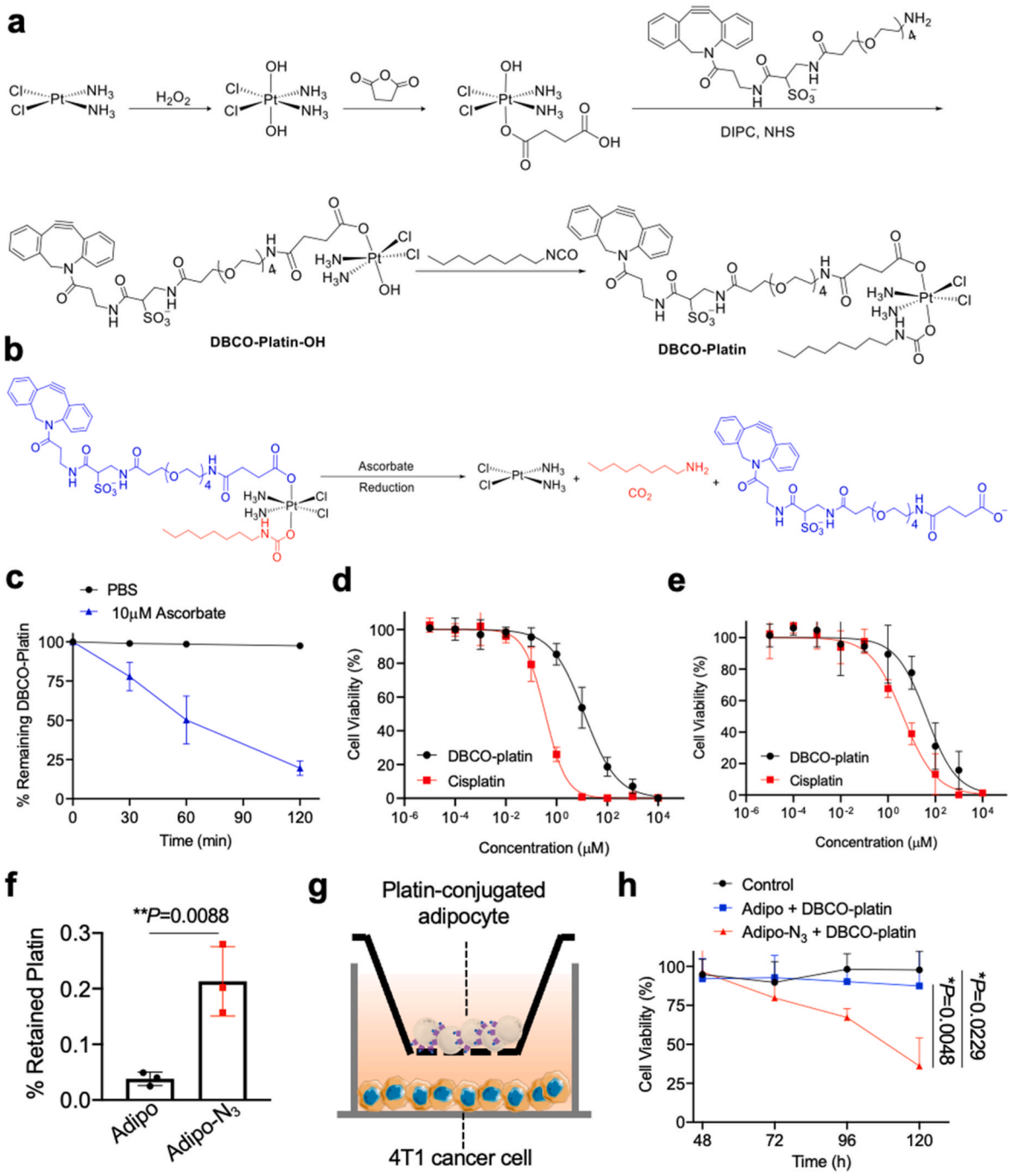

Fig. 4. Azido-labeled adipocytes enable conjugation of DBCO-platin and subsequent release of platin to kill surrounding tumor cells. (a) Synthetic route of DBCO-platin. (b) Degradation mechanism of DBCO-platin in the presence of ascorbate. (c) Degradation profiles of DBCO-platin in the presence or absence of 10 μM ascorbate, as determined via HPLC (detection wavelength: 291 nm). (d) Viability of 4T1 cells after 72-h incubation with DBCO-platin or cisplatin of varied concentrations. (e) Viability of 3T3-L1-differentiated adipocytes after 72-h incubation with DBCO-platin or cisplatin of varied concentrations. (f) Quantification of DBCO-platin conjugation to adipocytes by ICP-MS. 3T3-differentiated adipocytes were pretreated with Ac_4ManAz or PBS for three days and then incubated with DBCO-platin (25 μM) for 1 h. (g) Illustration of the transwell coculture study of platin-conjugated adipocytes and 4T1 cancer cells. (h) Viability of 4T1 cells at different times after the transwell cocultures with adipocytes. 4T1 cells incubated with PBS or adipocytes without conjugated drugs were used as controls. All the numerical data are presented as mean ± SD. Two-tailed Welch's *t*-test was used for (f) and one-way ANOVA with post hoc Fisher's LSD test was used for (h) ($0.01 < {}^{*}P \leq 0.05$; $0.001 < {}^{**}P \leq 0.01$; $0.0001 < {}^{***}P \leq 0.001$, ${}^{****}P \leq 0.0001$).

DBCO-platin showed a significantly higher expression level of pH2A.X, demonstrating that the cytotoxic effect is mainly attributed to DBCO-platin carried by adipocytes instead of the adipocyte itself (Figs. S6a–b).

2.5. Adipocyte-mediated prevention of post-surgical TNBC recurrence

After demonstrating the ability of azido-labeled adipocytes to capture and release drugs for cancer cell killing *in vitro*, we next studied whether azido-labeled primary adipocytes inoculated to the tumor resection site can mediate *in vivo* targeted delivery of DBCO-platin for

prevention of tumor recurrence. Luciferase-expressing 4T1 cells (500 k per mouse) were subcutaneously inoculated into Balb/c mice. When the tumor volume reached ~150 mm^3, tumors were surgically resected and primary adipocytes with or without Ac_4ManNAz pretreatment were injected into the surgical site. At 4 days post tumor resection, DBCO-platin or cisplatin was intravenously injected (Fig. 5a). Mice without drug treatment showed rapid tumor recurrence after the surgical resection of primary tumors (Fig. 5b). The combination of unlabeled adipocytes and DBCO-platin failed to exert any improvement in the prevention of tumor recurrence (Fig. 5b). Nevertheless, Adipo + DBCO-platin did result in a slightly prolonged animal survival and reduced metastases than the untreated group (Fig. 5b, Fig. S7b). In contrast, azido-labeled adipocytes coupled with DBCO-platin resulted in significantly improved prevention of 4T1 tumor recurrence (Fig. 5b), which could be attributed to adipocyte-mediated targeted delivery of drugs to the surgical site. It is noteworthy that tumor metastases occurred in most of the mice in this study, as evidenced by the bioluminescence signal in lung tissues (Fig. 5c, Fig. S7b). Compared to unlabeled adipocyte plus DBCO-platin, azido-labeled adipocytes coupled with DBCO-platin resulted in less metastases (Fig. 5c, Fig. S7b) and prolonged animal survival (Fig. 5d). However, the presence of metastases dramatically shortened the survival of mice and made it difficult to compare the ability of different therapies to prevent long-term tumor recurrence post surgery.

To minimize the occurrence of tumor metastases and enable long-time monitoring of tumor recurrence at the surgical site, in a separate study, we inoculated 100 k 4T1 cells into each mouse and performed the tumor surgery when the tumor volume reached ~50 mm^3 (Fig. 6a). Adipocytes with or without Ac_4ManNAz pretreatment were injected into the tumor resection site. At five days post tumor resection, DBCO-platin was intravenously injected. Mice without drug treatment again experienced rapid tumor recurrence (Fig. 6b–c). Both drug treatment groups showed much slower tumor recurrence (Fig. 6b–e). Compared to mice treated with unlabeled adipocytes and DBCO-platin, mice receiving azido-labeled adipocytes and DBCO-platin showed a significantly slower tumor growth rate (Fig. 6d–f). Azido-labeled adipocytes coupled with DBCO-platin also resulted in prolonged animal survival compared to all the other groups (Fig. 6g) without inducing any noticeable toxicity (Fig. 6h, Fig. S8). These experiments demonstrated that the grafted azido-labeled adipocytes could mediate targeted conjugation of DBCO-drugs for improved inhibition of tumor recurrence.

3. Discussion

Due to its low immunogenicity and association with various diseases, adipocyte is an attractive engineering target for drug delivery applications. However, existing adipocyte engineering methodologies have been largely limited to the physical adsorption of cargos [15,39]. For instance, loading of anticancer drugs into adipocytes was attempted via simple mixing. Adipocytes were also treated with plasmids or Cas9/gRNA complexes for genetic engineering [40,41]. These approaches inevitably suffer from limited efficiency due to the low endocytic activity of mature adipocytes. Conventional cell engineering approaches also include the binding of antibody-drug conjugates to specific surface receptors of cells, but the lack of characteristic receptors on adipocytes poses a significant challenge for developing adipocyte-targeting antibodies. The metabolic glycan labeling technology provides a facile method to modify surface glycoproteins and glycolipids of adipocytes with unique chemical tags (e.g., azido groups) [42–45], for subsequent targeted conjugation of cargos via efficient click chemistry. In principle, any cargo of interest, with simple DBCO modification, can readily be conjugated to azido-labeled adipocytes. It is noteworthy that DBCO-platin exhibits a reduced cytotoxic effect than free platin, which is consistent with the previous reports [23,25] and confers a high maximum tolerated dose and reduced systemic toxicity for DBCO-platin.

The ability to direct chemotherapeutics to the grafted adipose tissues at the tumor resection site holds promise to improve the clearance of residual tumor cells and prevention of tumor recurrence in the context of breast cancer surgery. While drugs can be loaded into fat tissues at the time of surgery, methods to enable the targeting of drugs to the grafted fat tissues hours or days after surgery are lacking. To adapt to the clinical

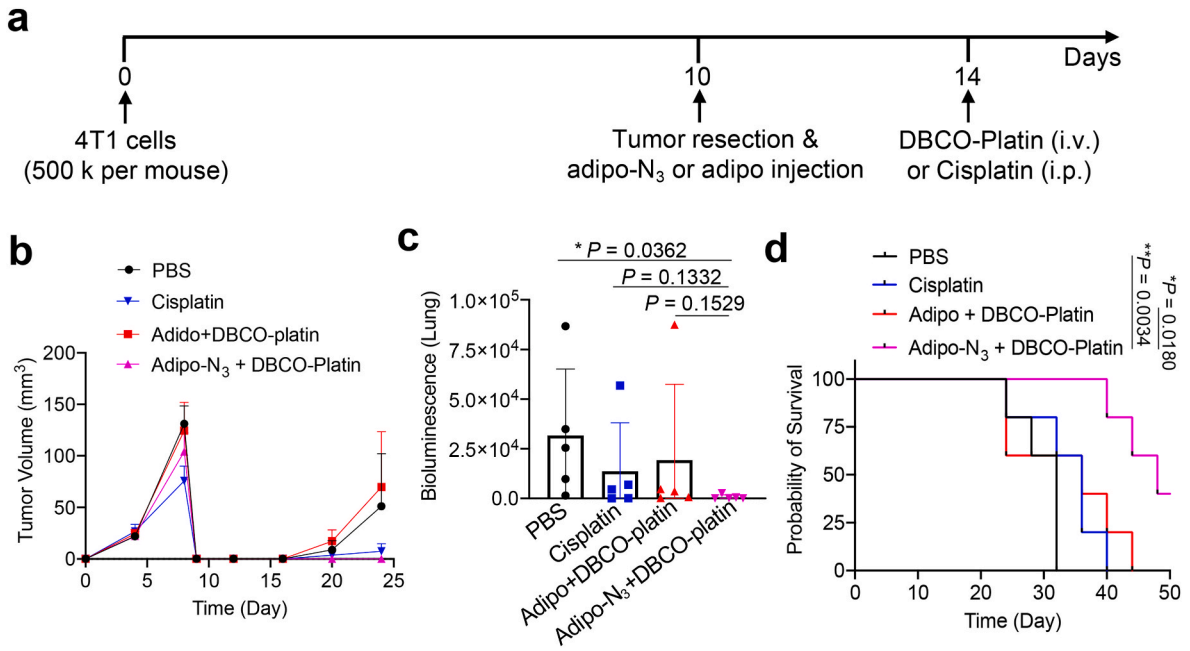

Fig. 5. Azido-labeled adipocytes enable targeted delivery of DBCO-platin to the tumor resection site for improved prevention of tumor recurrence. Azido-labeled primary adipocytes or control adipocytes were injected to the breast cancer resection site, followed by i.v. injection of DBCO-platin. (a) Timeframe of the efficacy study. (b) Average tumor volume for each group over the course of the tumor study. (c) Bioluminescence intensity of 4T1 lung metastases on day 24. (d) Kaplan–Meier plots for all groups. All the numerical data are presented as mean ± SD (one-way ANOVA with post hoc Fisher's LSD test was used; $0.01 < *P \leq 0.05$; $0.001 < **P \leq 0.01$; $0.0001 < ***P \leq 0.001$).

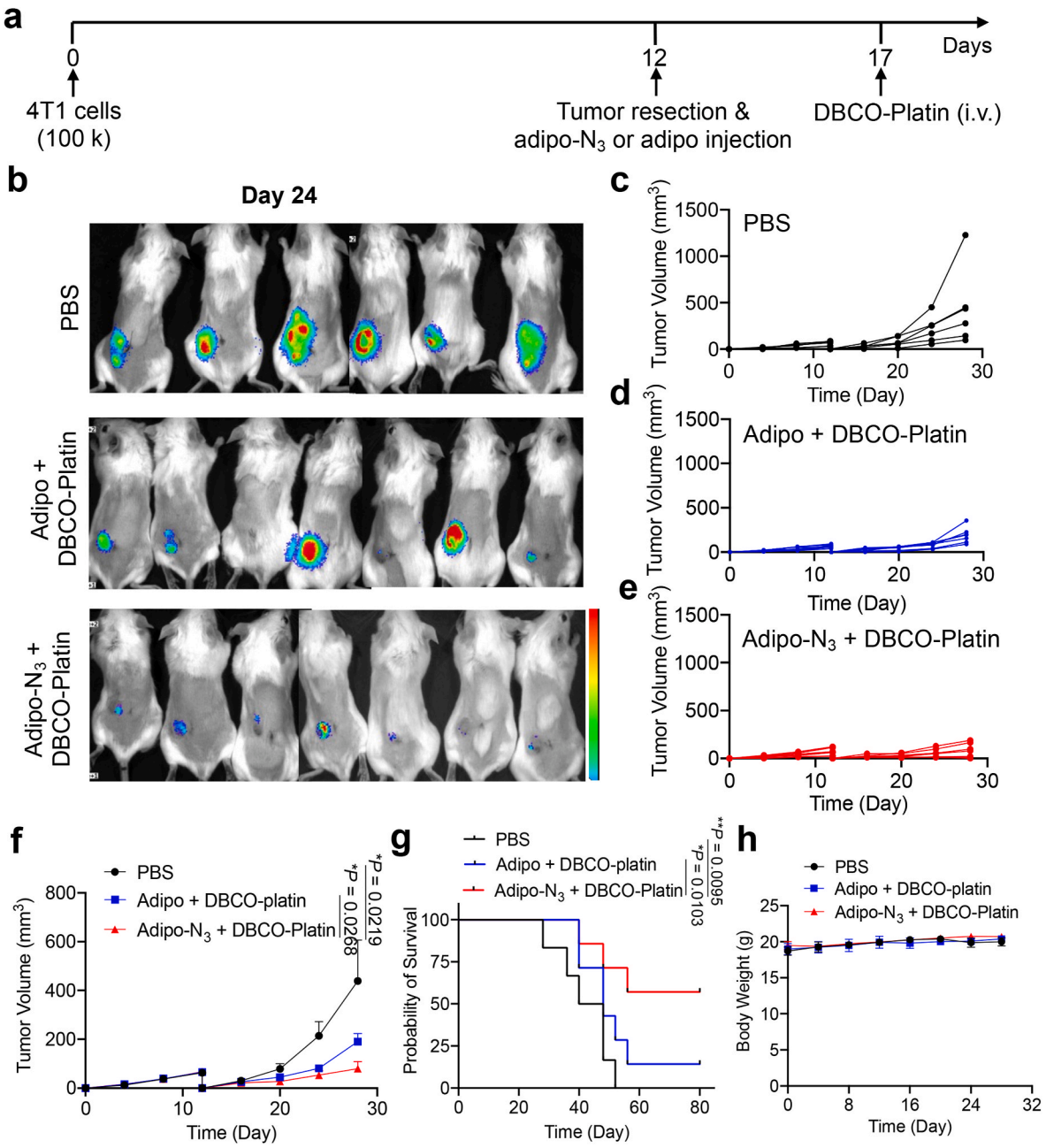

Fig. 6. Azido-labeled adipocytes coupled with DBCO-platin improves prevention of post-surgical tumor recurrence. (a) Timeframe of the tumor resection study. Luciferase-expressing 4T1 TNBC cells were inoculated into the flank of the mice on day 0. Tumor surgery was performed and adipocytes were grafted to the surgical site on day 12. DBCO-platin was intravenously injected on day 17. (b) *In vivo* bioluminescence imaging of mice on day 24. (c–e) Individual tumor volume curves for each group. (f) Average tumor volume of different groups over the course of the tumor study. (g) Kaplan–Meier plots for all groups. (h) Average body weight of mice over the course of the tumor study. Data in (f) are presented as mean ± SEM and data in (h) are presented as mean ± SD (one-way ANOVA with post hoc Fisher's LSD test was used; $0.01 < {}^{*}P \leq 0.05$; $0.001 < {}^{**}P \leq 0.01$; $0.0001 < {}^{***}P \leq 0.001$).

practice of breast cancer surgery, we tested the feasibility of immersing primary adipocytes in a solution of azido-sugar for a short duration (2 h) and continuing the metabolic labeling process *in vivo* after grafting to the surgical site. As a result, grafted primary adipocytes were successfully labeled with azido groups and enabled targeted conjugation of subsequently intravenously administered DBCO-cargo. Our *in vitro* drug conjugation study using 3T3-L1-differentiated adipocytes showed that 0.2% of DBCO-platin (25 μM, 100 μL) can be covalently captured by azido-labeled adipocytes (10,000 cells) via click chemistry (Fig. 4f), which corresponds to 3×10^8 platin molecules per cell. This is indeed a considerable amount of drug per adipocyte to realize the therapeutic potential of our targetable drug depot approach. The long-term stability of azido groups expressed by mature adipocytes enable the targeting of DBCO-cargos days after the surgery. We envision various applications of this primary adipocyte targeting technology in the context of cancer and other diseases.

4. Conclusion

To conclude, we have developed an *in vivo* targetable adipocyte-based drug depot for the prevention of post-surgical cancer recurrence. Primary adipocytes can be metabolically labeled with azido groups via metabolic glycoengineering processes of Ac_4ManNAz. In compliance with the clinical practice, we showed that the simple

incubation of primary adipocytes with azido-sugar for 2 h prior to transplantation could result in azido-labeled adipocytes *in vivo*. These azido-tagged primary adipocytes then enable targeted conjugation of DBCO-cargos via efficient click chemistry. We further demonstrated that azido-labeled adipocytes grafted to the tumor resection site can mediate the targeting of DBCO-drugs for improved prevention of tumor recurrence in a 4T1 TNBC model. Our approach will greatly facilitate the development of adipocyte-based therapies in the context of cancer and other diseases.

5. Methods

5.1. Materials and instrumentation

D-Mannosamine hydrochloride, DBCO-Cy5, sodium azide, chloroacetic anhydride, acetic anhydride, cisplatin, DBCO-*sulfo*-amine, L-luciferin potassium, octyl isocyanate, MTT, and other chemical reagents are purchased from Sigma Aldrich (St. Louis, MO, USA) unless otherwise noted. High-performance liquid chromatography (HPLC) analysis was performed on a Shimadzu CBM-20A system (Shimadzu, Kyoto, Japan) equipped with an SPD-20A PDA detector (190–800 nm), an RF-20A fluorescence detector, and an analytical C18 column (Shimadzu, 3 μm, 50 × 4.6 mm, Kyoto, Japan). Preparative HPLC was performed on a CombiFlash®Rf system (Teledyne ISCO, Lincoln, NE, USA) equipped with a RediSep®Rf HP C18 column (Teledyne ISCO, 30 g, Lincoln, NE, USA). Lyophilization was conducted in a Labconco FreeZone lyophilizer (Kansas City, MO, USA). Nuclear Magnetic Resonance (NMR) spectra were recorded on a Varian U500 (500 MHz) or VXR500 (500 MHz), or a Bruker Carver B500 (500 MHz) spectrometer. Electrospray ionization (ESI) mass spectra were obtained from a Waters ZMD Quadrupole Instrument (Waters, Milford, MA, USA). Flow cytometry analysis was conducted on an Attune NxT flow cytometer and analyzed on FCS Express v6 and v7. Confocal laser scanning microscopy (CLSM) images were taken by using a Zeiss LSM 700 Confocal Microscope (Carl Zeiss, Thornwood, NY, USA). *In vivo* and *ex vivo* images of animals and tissues were taken on a Bruker In Vivo Imaging System (Bruker, Billerica, MA, USA).

5.2. Cell line and animals

3T3-L1 and 4T1 cell lines were purchased from the American Type Culture Collection (Manassas, VA, USA). 4T1 cells were cultured in RPMI-1640 media containing 10% FBS, 100 units/mL Penicillin G and 100 μg/mL streptomycin at 37 °C in a 5% CO_2 humidified incubator. 3T3-L1 cells were cultured in DMEM media containing 10% bovine calf serum (Gibco), 100 units/mL Penicillin G and 100 μg/mL streptomycin at 37 °C in a 5% CO_2 humidified incubator. Balb/c mice were purchased from the Jackson Laboratory (Bar Harbor, ME, USA). Feed and water were available ad libitum. Artificial light was provided in a 12 h/12 h cycle. All procedures involving animals were done in compliance with the National Institutes of Health and Institutional guidelines with approval from the Institutional Animal Care and Use Committee at the University of Illinois at Urbana-Champaign.

5.3. Synthesis of Ac_4ManNAz

D-Mannosamine hydrochloride (1.0 mmol) and triethylamine (1.0 mmol) were dissolved in methanol, followed by the addition of *N*-(2-azidoacetyl) succinimide (1.2 mmol). The mixture was stirred at room temperature for 24 h to yield *N*-(2-azidoacetyl)mannosamine, which was directly used for the next step without purification. Solvent was removed under reduced pressure and the residue was re-dissolved in pyridine. Acetic anhydride was added and the reaction mixture was stirred at room temperature for another 24 h. After removal of the solvent, the crude product was purified by silica gel column chromatography using ethyl acetate/hexane (1/1, v/v) as the eluent to yield a white solid (1/1 α/β isomers). ^{1}H NMR ($CDCl_3$, 500 MHz): δ (ppm) 6.66&6.60 (d, J = 9.0 Hz, 1H, C(O)N*H*CH), 6.04&6.04 (d, 1H, J = 1.9 Hz, NHCHC*H*O), 5.32–5.35&5.04–5.07 (dd, J = 10.2, 4.2 Hz, 1H, CH_2CHC*H*CH), 5.22&5.16 (t, J = 9.9 Hz, 1H, CH_2CHCHC*H*), 4.60–4.63&4.71–4.74 (m, 1H, NHC*H*CHO), 4.10–4.27 (m, 2H, C*H*$_2$CHCHCH), 4.07 (m, 2H, C(O)C*H*$_2$$N_3$), 3.80–4.04 (m, 1H, CH_2C*H*CHCH), 2.00–2.18 (s, 12H, C*H*$_3$C(O)). ^{13}C NMR ($CDCl_3$, 500 MHz): δ (ppm) 170.7, 170.4, 170.3, 169.8, 168.6, 168.3, 167.5, 166.9, 91.5, 90.5, 73.6, 71.7, 70.5, 69.1, 65.3, 65.1, 62.0, 61.9, 52.8, 52.6, 49.9, 49.5, 21.1, 21.0, 21.0, 20.9, 20.9, 20.9, 20.8. ESI MS (m/z): calculated for $C_{16}H_{22}N_4O_{10}Na$ $[M+Na]^+$ 453.1, found 453.1.

5.4. In vivo metabolic labeling and targeting of primary adipocytes

Abdominal fat tissues under the mammary gland in 8-week C57BL/6 female mice were collected via blunt dissection. The adipose tissue was rinsed with PBS, minced into fragments of ~1 mm, and treated with collagenase at 37 °C for 1 h. The cell suspension was then centrifuged at 150 g for 8 min. Adipocytes in the supernatants were collected, while the stromal vascular fraction (SVF) in the bottom pellet was discarded. The collected adipocytes were incubated with Ac_4ManNAz (100 μM) or PBS for 2 h. Cells were simultaneously stained with Calcein AM (500 nM) for 2 h. After washing, 10^7 Ac_4ManNAz-labeled adipocytes were inoculated to the left mammary fat pad of C57BL/6 mice. Unlabeled adipocytes were inoculated into the right mammary fat pad. At 48 h, mice were euthanized and fat tissues were harvested from the mammary fat pad. Half of the tissue was homogenized into single-cell suspension, incubated with DBCO-Cy5 (20 μM), and analyzed on a flow cytometer. Another half of the tissue was embedded into OCT and sectioned with a thickness of 5 μm. The tissue sections were stained with DBCO-Cy5 (20 μM) and Hoechst 33342 for 10 min, washed, and imaged under a Zeiss LSM700 confocal microscope. For the targeting study, at 48 h post inoculation of adipocytes, DBCO-Cy5 (5 mg/kg) was intravenously administrated into mice. Mice were then imaged using the IVIS Imaging System at several given time pointes with an excitation/emission filter of 640/700 nm. After euthanizing the mice, major organs including the fat tissues were harvested and imaged with IVIS Imaging System *ex vivo*.

5.5. Synthesis of DBCO-Platin-OH

DBCO-Platin-OH $[Pt(NH_3)_2Cl_2(OH)(O_2CCH_2CH_2CO_2H)]$ was synthesized according to the previously reported method [42]. $[Pt(NH_3)_2Cl_2(OH)(O_2CCH_2CH_2CO_2H)]$ (500 mg, 1.15 mmol), *N*-hydroxysuccinimide (265 mg, 2.30 mmol), N,N′-diisopropylcarbodiimide (215 mg, 1.73 mmol) were dissolved in anhydrous dimethyl sulfoxide and stirred for 3 h. DBCO-sulfo-amine (622 mg, 0.92 mmol) and triethylamine (93 mg, 0.92 mmol) were then added, stirred for another 10 min, and quenched with ammonium bicarbonate solution. The crude product was purified on a preparative CombiFlash®Rf system to yield a light yellow powder (315 mg, 31% yield). 1H NMR (500 MHz, DMSO-d_6). δ 7.89 (m, 2H), 7.62–7.44 (m, 4H), 7.43–7.21 (m, 4H), 6.01 (br, 6H), 5.20 (dd, J = 13.5, 3.0 Hz, 1H), 4.22 (m, 1H), 3.54 (d, J = 14.0 Hz), 3.42 (m, 13H), 3.36 (t, J = 5.5 Hz, 2H), 3.15 (m, 2H), 3.09–2.86 (m, 4H), 2.77–2.67 (m, 2H), 2.35 (t, J = 25.8 Hz, 2H), 2.30–2.24 (m, 6H). LRMS (ESI) $[M + H]^+$ Calculatedd for $C_{36}H_{52}Cl_2N_6O_{14}PtS$: 1090.3, found: 1090.7.

5.6. Synthesis of DBCO-Platin

In a 7 mL dark vial, DBCO-Platin-OH (200 mg, 0.18 mmol) was dissolved with anhydrous dimethyl sulfoxide. Octyl isocyanate (30.9 mg, 0.20 mmol) was added, and the mixture was stirred at 40 °C for 5 h. The crude product was purified on a preparative CombiFlash®Rf system to yield a light yellow powder (161 mg, 71% yield). ^{1}H NMR (500 MHz, DMSO-d_6). δ 7.90 (m, 2H), 7.67–7.46 (m, 4H), 7.45–7.23 (m, 4H), 5.87 (br, 6H), 5.03 (dd, J = 14.1, 3.5 Hz, 1H), 4.20 (m, 1H), 3.54–3.30 (m, 15

H), 2.92 (d, $J = 13.1$ Hz, 4H), 2.80–2.51 (m, 4H), 2.39 (t, $J = 29.6$ Hz, 2H), 2.34–2.17 (m, 6H), 1.22 (m, 16H), 0.83 (t, $J = 6.9$ Hz, 3H). LRMS (ESI) $[M + H]^+$ Calcd for $C_{45}H_{70}Cl_2N_7O_{15}PtS$: 1244.4, found: 1244.5.

5.7. Degradation of DBCO-platin

DBCO-Platin was added to a buffer solution (5 mM NH_4HCO_3 in H_2O) containing ascorbic acid (10 μM). The mixture was incubated at 37 °C. 1 mL aliquots of the solution were taken out for HPLC measurements at selected time points. DBCO-platin was detected with a PDA detector ($\lambda = 291$ nm).

5.8. Cytotoxicity of DBCO-platin and cisplatin

4T1 cells were seeded at a density of 2×10^4 per well into a 96-well plate and incubated with varied concentrations of DBCO-platin or cisplatin. After 72 h, the viability of cells was determined via the standard MTT assay.

5.9. Differentiation of 3T3-L1 cells

3T3-L1 cells were cultured to 70% confluency in full DMEM media. The medium was removed, and an MDI induction medium containing IBMX (0.5 mM), dexamethasone (1 μM), and insulin (10 μg/mL) was added. Cells were incubated for three days. After removing the MDI induction medium, insulin media (10 μg/mL insulin in DMEM) was added. Cells were incubated for another three days. The insulin medium was then removed, and cells were maintained in the DMEM medium. The differentiated adipocytes were verified by Oil Red staining, morphology change, and lipid droplet structures.

5.10. Quantification of adipocyte-conjugated DBCO-Platin

3T3-L1-differentiated adipocytes were incubated with Ac_4ManNAz (50 μM) at 37 °C for 72 h. After washing with PBS, cells were incubated with DBCO-Platin (25 μM) for 1 h. After washing, the adipocytes were treated with 300 μL of SDS lysis buffer, diluted with 700 μL of 1 M nitric acid solution, and analyzed via ICP-MS. The standard samples were prepared by mixing blank cell lysates with 0, 1, 2, 5, or 10 ppb Pt, and then subjected to ICP-MS measurement.

5.11. Transwell coculture study of adipocytes and cancer cells

3T3-L1-differentiated adipocytes were cultured in a transwell insert placed in a 12-well plate. Cells were treated with Ac_4ManNAz (50 μM) for 72 h and then DBCO-platin for 1 h, while adipocytes without Ac_4ManNAz treatment were used as controls. Adipocytes were washed with PBS, and the transwell insert was transferred to a 12-well plate pre-seeded with 5×10^5 4T1 cells. After the designated coculture times, the viability of 4T1 cells was measured via the standard MTT assay.

5.12. pH2AX staining

3T3-L1-differentiated adipocytes were incubated with Ac_4ManNAz (50 μM) at 37 °C for 72 h. After washing with PBS, cells were incubated with DBCO-Platin (50 μM) for 2 h. After washing, the platin-conjugated adipocytes and control adipocytes (without DBCO-platin conjugation) were lifted, counted, and seeded (10^5 per well) to a 48-well plate pre-seeded with 5×10^4 4T1 cells in adipocyte maintenance media. 4T1 cells cocultured with media containing DBCO-Platin (50 μM) or PBS were used as controls. After 72 h, the adipocytes were washed away with PBS. The 4T1 cells were lifted, washed, stained with the fixable viability dye (eBioscience) and phospho-Histone H2A.X antibody (CR55T33, eBioscience), and analyzed on a flow cytometer.

5.13. Tumor resection study

Luciferase-expressing 4T1 cells (5×10^5 cells per mouse) suspended in Matrigel/HBSS (30 μL, 1:1, v:v) were subcutaneously injected into the right flank of 8-week Balb/c mice. When the tumor size reached ~150 mm^3, mice were randomly divided into four groups: PBS, cisplatin, adipocyte + DBCO-platin, and azido-labeled adipocyte + DBCO-platin. Tumors were surgically removed under anesthesia, and 10^7 Ac_4ManNAz-treated or untreated adipocytes (from Balb/c mice) were inoculated to the surgical site. At 4 days post tumor resection, DBCO-platin (40 mg/kg, 200 μL) was intravenously injected into group 3 and group 4 mice. Cisplatin (5 mg/kg, 200 μL) was intraperitoneally injected into group 2 mice. The tumor volume and body weight of mice were measured every other day. The tumor volume was calculated using the formula (length) × (width) [2]/2, with both length and width measured by a caliper, where the long axis diameter was regarded as the length, and the short axis diameter was regarded as the width. Tumor recurrence and lung metastases were monitored via bioluminescence imaging of Balb/c mice using the IVIS imaging system. In a separate study that aims to minimize the occurrence of metastasis, luciferase-expressing 4T1 cells (100 k per mouse, suspended in Matrigel/HBSS (30 μL, 1:1/v:v)) were subcutaneously injected into the right flank of Balb/c mice. When the tumor size reached 50 mm^3, mice were randomly divided into three groups: PBS; adipocyte + DBCO-platin; azido-labeled adipocyte + DBCO-platin. Tumors were surgically removed, and 10^7 Ac_4ManNAz-treated or untreated adipocytes were inoculated to the surgical site. At 5 days post tumor resection, DBCO-platin (40 mg/kg) was intravenously injected. At selected times, bioluminescence imaging of mice, with intraperitoneal injection of potassium luciferin, was taken on the IVIS instrument, in order to monitor the recurrence and growth of tumors. For mice showing subcutaneous tumors, the tumor volume and mouse body weight were measured every other day. The subcutaneous tumor volume was calculated using the formula (length) × (width) [2]/2, where the long axis diameter was regarded as the length, and the short axis diameter was regarded as the width, with both length and width measured by a caliper. After euthanizing the mice, major organs were collected, fixed with 10% formalin solution, embedded in paraffin, and stained with H&E for pathological analysis.

5.14. Statistical analysis

Statistical analysis was performed using GraphPad Prism v6 and v8. Sample variance was tested using the F test. For samples with equal variance, the significance between the groups was analyzed by a two-tailed student's t-test. For samples with unequal variance, a two-tailed Welch's *t*-test was performed. For multiple comparisons, a one-way analysis of variance (ANOVA) with a post hoc Fisher's LSD test was used. The results were deemed significant at $0.01 < {}^*P \leq 0.05$, highly significant at $0.001 < {}^{**}P \leq 0.01$, and extremely significant at *** $0.01 < P \leq 0.001$, **** $P < 0.0001$.

CRediT authorship contribution statement

Yang Bo: Writing – review & editing, Writing – original draft, Methodology, Investigation, Formal analysis. **Yueji Wang:** Writing – review & editing, Investigation, Formal analysis. **Joonsu Han:** Writing – review & editing, Investigation. **Rimsha Bhatta:** Writing – review & editing, Investigation. **Yusheng Liu:** Writing – review & editing, Investigation. **Dhyanesh Baskaran:** Writing – review & editing, Investigation. **Jiadiao Zhou:** Writing – review & editing, Investigation. **Hua Wang:** Writing – review & editing, Supervision, Funding acquisition, Formal analysis, Conceptualization.

Declaration of competing interest

The authors declare that they have no known competing financial

interests or personal relationships that could have appeared to influence the work reported in this paper.

Data availability

Data will be made available on request.

Acknowledgments

The authors would like to acknowledge the financial support from NSF DMR 2143673 CAR, NIH R01CA274738, NIH R21CA270872, and the start-up package from the Department of Materials Science and Engineering at the University of Illinois at Urbana-Champaign and the Cancer Center at Illinois. Research reported in this publication was supported by the Cancer Scholars for Translational and Applied Research (C*STAR) Program sponsored by the Cancer Center at Illinois and the Carle Cancer Center under Award Number CST EP012023.

Appendix A. Supplementary data

Supplementary data to this article can be found online at https://doi.org/10.1016/j.mtbio.2024.101020.

References

[1] G. Carioli, M. Malvezzi, T. Rodriguez, P. Bertuccio, E. Negri, C. La Vecchia, Trends and predictions to 2020 in breast cancer mortality: Americas and Australasia, Breast 37 (2018) 163–169.
[2] B. Fisher, S. Anderson, C.K. Redmond, N. Wolmark, D.L. Wickerham, W.M. Cronin, Reanalysis and results after 12 years of follow-up in a randomized clinical trial comparing total mastectomy with lumpectomy with or without irradiation in the treatment of breast cancer, N. Engl. J. Med. 333 (22) (1995) 1456–1461.
[3] B.D. Lehmann, J.A. Bauer, X. Chen, M.E. Sanders, A.B. Chakravarthy, Y. Shyr, J. A. Pietenpol, Identification of human triple-negative breast cancer subtypes and preclinical models for selection of targeted therapies, J. Clin. Invest. 121 (7) (2011) 2750–2767.
[4] K.A. Won, C. Spruck, Triple-negative breast cancer therapy: Current and future perspectives, Int. J. Oncol. 57 (6) (2020) 1245–1261.
[5] A.C. Chiang, J. Massagué, Molecular basis of metastasis, N. Engl. J. Med. 359 (26) (2008) 2814–2823.
[6] J.W. Uhr, K. Pantel, Controversies in clinical cancer dormancy, Proc. Natl. Acad. Sci. USA 108 (30) (2011) 12396–12400.
[7] R. Dent, M. Trudeau, K.I. Pritchard, W.M. Hanna, H.K. Kahn, C.A. Sawka, L. A. Lickley, E. Rawlinson, P. Sun, S.A. Narod, Triple-negative breast cancer: clinical features and patterns of recurrence, Clin. Cancer Res. 13 (15) (2007) 4429–4434.
[8] O. Kaidar-Person, P. Poortmans, B.V. Offersen, S. Siesling, M. Sklair-Levy, I. Meattini, D. de Ruysscher, T. Kühn, L.J. Boersma, Spatial location of local recurrences after mastectomy: a systematic review, Breast Cancer Res. Treat. 183 (2) (2020) 263–273.
[9] Y. Qi, H. Min, A. Mujeeb, Y. Zhang, X. Han, X. Zhao, G.J. Anderson, Y. Zhao, G. Nie, Injectable hexapeptide hydrogel for localized chemotherapy prevents breast cancer recurrence, ACS Appl. Mater. Interfaces 10 (8) (2018) 6972–6981.
[10] Y. Brudno, M.J. Pezone, T.K. Snyder, O. Uzun, C.T. Moody, M. Aizenberg, D. J. Mooney, Replenishable drug depot to combat post-resection cancer recurrence, Biomaterials 178 (2018) 373–382.
[11] H. Wang, A.J. Najibi, M.C. Sobral, B.R. Seo, J.Y. Lee, D. Wu, A.W. Li, C.S. Verbeke, D.J. Mooney, Biomaterial-based scaffold for in situ chemo-immunotherapy to treat poorly immunogenic tumors, Nat. Commun. 11 (1) (2020) 5696.
[12] J. Cortes, D.W. Cescon, H.S. Rugo, Z. Nowecki, S.-A. Im, M.M. Yusof, C. Gallardo, O. Lipatov, C.H. Barrios, E. Holgado, Pembrolizumab plus chemotherapy versus placebo plus chemotherapy for previously untreated locally recurrent inoperable or metastatic triple-negative breast cancer (KEYNOTE-355): a randomised, placebo-controlled, double-blind, phase 3 clinical trial, Lancet 396 (10265) (2020) 1817–1828.
[13] Y. Wu, Y. Yao, J. Zhang, H. Gui, J. Liu, J. Liu, Tumor-targeted injectable double-Network hydrogel for prevention of breast cancer recurrence and Wound Infection via Synergistic Photothermal and Brachytherapy, Adv. Sci. 9 (24) (2022) 2200681.
[14] Y. Chao, L. Xu, C. Liang, L. Feng, J. Xu, Z. Dong, L. Tian, X. Yi, K. Yang, Z. Liu, Combined local immunostimulatory radioisotope therapy and systemic immune checkpoint blockade imparts potent antitumour responses, Nat. Biomed. Eng. 2 (8) (2018) 611–621.
[15] D. Wen, J. Wang, G. Van Den Driessche, Q. Chen, Y. Zhang, G. Chen, H. Li, J. Soto, M. Liu, M. Ohashi, Adipocytes as anticancer drug delivery depot, Matter 1 (5) (2019) 1203–1214.
[16] R. Munteanu, A. Onaciu, C. Moldovan, A.-A. Zimta, D. Gulei, A.V. Paradiso, V. Lazar, I. Berindan-Neagoe, Adipocyte-based cell therapy in oncology: the role of cancer-associated adipocytes and their reinterpretation as delivery platforms, Pharmaceutics 12 (5) (2020) 402.
[17] S.S. Sharath, J. Ramu, S.V. Nair, S. Iyer, U. Mony, J. Rangasamy, Human adipose tissue derivatives as a potent native biomaterial for tissue regenerative therapies, Tissue Engineering and Regenerative Medicine 17 (2) (2020) 123–140.
[18] J. Anampa, D. Makower, J.A. Sparano, Progress in adjuvant chemotherapy for breast cancer: an overview, BMC Med. 13 (1) (2015) 1–13.
[19] M. Gieni, R. Avram, L. Dickson, F. Farrokhyar, P. Lovrics, S. Faidi, N. Sne, Local breast cancer recurrence after mastectomy and immediate breast reconstruction for invasive cancer: a meta-analysis, Breast 21 (3) (2012) 230–236.
[20] J.M. Simons, J.G. Jacobs, J.P. Roijers, M.A. Beek, L.J. Boonman-de Winter, A. M. Rijken, P.D. Gobardhan, J.H. Wijsman, E. Tetteroo, J.B. Heijns, Disease-free and overall survival after neoadjuvant chemotherapy in breast cancer: breast-conserving surgery compared to mastectomy in a large single-centre cohort study, Breast Cancer Res. Treat. 185 (2) (2021) 441–451.
[21] Z.-Y. Wu, H.-J. Kim, J.-W. Lee, I.-Y. Chung, J.-S. Kim, S.-B. Lee, B.-H. Son, J.-S. Eom, S.-B. Kim, K.H. Jung, Long-term oncologic outcomes of immediate breast reconstruction vs conventional mastectomy alone for breast cancer in the setting of neoadjuvant chemotherapy, JAMA surgery 155 (12) (2020) 1142–1150.
[22] H. Wang, D.J. Mooney, Metabolic glycan labelling for cancer-targeted therapy, Nat. Chem. 12 (12) (2020) 1102–1114.
[23] H. Wang, R. Wang, K. Cai, H. He, Y. Liu, J. Yen, Z. Wang, M. Xu, Y. Sun, X. Zhou, Q. Yin, L. Tang, I.T. Dobrucki, L.W. Dobrucki, E.J. Chaney, S.A. Boppart, T.M. Fan, S. Lezmi, X. Chen, L. Yin, J. Cheng, Selective in vivo metabolic cell-labeling-mediated cancer targeting, Nat. Chem. Biol. 13 (4) (2017) 415–424.
[24] H. Wang, M.C. Sobral, D.K.Y. Zhang, A.N. Cartwright, A.W. Li, M.O. Dellacherie, C. M. Tringides, S.T. Koshy, K.W. Wucherpfennig, D.J. Mooney, Metabolic labeling and targeted modulation of dendritic cells, Nat. Mater. 19 (2020) 1244–1252.
[25] Y. Bo, J. Zhou, K. Cai, Y. Wang, Y. Feng, W. Li, Y. Jiang, S.H. Kuo, J. Roy, C. Anorma, Leveraging intracellular ALDH1A1 activity for selective cancer stem-like cell labeling and targeted treatment via in vivo click reaction, Proc. Natl. Acad. Sci. USA 120 (36) (2023) e2302342120.
[26] P.V. Chang, J.A. Prescher, E.M. Sletten, J.M. Baskin, I.A. Miller, N.J. Agard, A. Lo, C.R. Bertozzi, Copper-free click chemistry in living animals, Proc. Natl. Acad. Sci. USA 107 (5) (2010) 1821–1826.
[27] J.A. Codelli, J.M. Baskin, N.J. Agard, C.R. Bertozzi, Second-generation difluorinated cyclooctynes for copper-free click chemistry, J. Am. Chem. Soc. 130 (34) (2008) 11486–11493.
[28] H. Wang, Y. Bo, Y. Liu, M. Xu, K. Cai, R. Wang, J. Cheng, In vivo cancer targeting via glycopolyester nanoparticle mediated metabolic cell labeling followed by click reaction, Biomaterials (2019) 119305.
[29] H. Wang, Immune cell homing biomaterials for immunotherapy, Acc. Mater. Res. 1 (3) (2020) 172–174.
[30] J. Han, R. Bhatta, Y. Liu, Y. Bo, A. Elosegui-Artola, H. Wang, Metabolic glycan labeling immobilizes dendritic cell membrane and enhances antitumor efficacy of dendritic cell vaccine, Nat. Commun. 14 (1) (2023) 5049.
[31] Y. Bo, Y. Jiang, K. Chen, K. Cai, W. Li, J. Roy, Y. Bao, J. Cheng, Targeting infected host cells in vivo via responsive azido-sugar mediated metabolic cell labeling followed by click reaction, Biomaterials 238 (2020) 119843.
[32] J. Oeckl, A. Bast-Habersbrunner, T. Fromme, M. Klingenspor, Y. Li, Isolation, culture, and functional analysis of murine thermogenic adipocytes, STAR protocols 1 (3) (2020) 100118.
[33] D.P. Silver, A.L. Richardson, A.C. Eklund, Z.C. Wang, Z. Szallasi, Q. Li, N. Juul, C.-O. Leong, D. Calogrias, A. Buraimoh, Efficacy of neoadjuvant Cisplatin in triple-negative breast cancer, J. Clin. Oncol. 28 (7) (2010) 1145.
[34] Y.-R. Zheng, K. Suntharalingam, T.C. Johnstone, H. Yoo, W. Lin, J.G. Brooks, S. J. Lippard, Pt (IV) prodrugs designed to bind non-covalently to human serum albumin for drug delivery, J. Am. Chem. Soc. 136 (24) (2014) 8790–8798.
[35] M.D. Hall, T.W. Hambley, Platinum (IV) antitumour compounds: their bioinorganic chemistry, Coord. Chem. Rev. 232 (1–2) (2002) 49–67.
[36] T.C. Johnstone, J.J. Wilson, S.J. Lippard, Monofunctional and higher-valent platinum anticancer agents, Inorganic chemistry 52 (21) (2013) 12234–12249.
[37] S. Morrison, S.L. McGee, 3T3-L1 adipocytes display phenotypic characteristics of multiple adipocyte lineages, Adipocyte 4 (4) (2015) 295–302.
[38] A.J. Wilson, E. Holson, F. Wagner, Y.-L. Zhang, D.M. Fass, S.J. Haggarty, S. Bhaskara, S.W. Hiebert, S.L. Schreiber, D. Khabele, The DNA damage mark pH2AX differentiates the cytotoxic effects of small molecule HDAC inhibitors in ovarian cancer cells, Cancer Biol. Ther. 12 (6) (2011) 484–493.
[39] D. Wen, T. Liang, G. Chen, H. Li, Z. Wang, J. Wang, R. Fu, X. Han, T. Ci, Y. Zhang, Adipocytes Encapsulating Telratolimod Recruit and Polarize tumor-associated Macrophages for cancer immunotherapy, Adv. Sci. 10 (5) (2023) 2206001.
[40] E. Tsagkaraki, S.M. Nicoloro, T. DeSouza, J. Solivan-Rivera, A. Desai, L.M. Lifshitz, Y. Shen, M. Kelly, A. Guilherme, F. Henriques, CRISPR-enhanced human adipocyte browning as cell therapy for metabolic disease, Nat. Commun. 12 (1) (2021) 6931.
[41] C.-H. Wang, M. Lundh, A. Fu, R. Kriszt, T.L. Huang, M.D. Lynes, L.O. Leiria, F. Shamsi, J. Darcy, B.P. Greenwood, CRISPR-engineered human brown-like adipocytes prevent diet-induced obesity and ameliorate metabolic syndrome in mice, Sci. Transl. Med. 12 (558) (2020) eaaz8664.
[42] R. Xie, L. Dong, Y. Du, Y. Zhu, R. Hua, C. Zhang, X. Chen, In vivo metabolic labeling of sialoglycans in the mouse brain by using a liposome-assisted bioorthogonal reporter strategy, Proc. Natl. Acad. Sci. USA 113 (19) (2016) 5173–5178.

[43] E. Saxon, C.R. Bertozzi, Cell surface engineering by a modified Staudinger reaction, Science 287 (5460) (2000) 2007–2010.
[44] R. Xie, L. Dong, R. Huang, S. Hong, R. Lei, X. Chen, Targeted imaging and proteomic analysis of tumor-associated glycans in living animals, Angew. Chem. Int. Ed. 53 (51) (2014) 14082–14086.
[45] C. Agatemor, M.J. Buettner, R. Ariss, K. Muthiah, C.T. Saeui, K.J. Yarema, Exploiting metabolic glycoengineering to advance healthcare, Nat. Rev. Chem 3 (10) (2019) 605–620.